Available online at www.sciencedirect.com

SciVerse ScienceDirect

Ceramics International 38 (2012) 5281–5285

CERAMICS INTERNATIONAL

www.elsevier.com/locate/ceramint

Short communication

Nb_2O_5 doping effect on electrical properties of $ZnO–V_2O_5–Mn_3O_4$ varistor ceramics

Choon-W. Nahm *

Semiconductor Ceramics Laboratory, Department of Electrical Engineering, Dongeui University, Busan 614-714, Republic of Korea

Received 26 January 2012; accepted 16 February 2012
Available online 25 February 2012

Abstract

The microstructure and electrical properties of ternary $ZnO–V_2O_5–Mn_3O_4$ varistor ceramics modified with Nb_2O_5 were systematically investigated for different amounts of Nb_2O_5. The average grain size for Nb_2O_5-doped ceramics was larger than Nb_2O_5-free ceramics and it was in the range of 6.64–7.27 μm. The sintered density of pellets increased from 5.50 to 5.54 g/cm^3 as the Nb_2O_5 amount increased. The breakdown field increased from 947 to 4521 V/cm with an increase in the amount of Nb_2O_5, whereas a further addition caused it to decrease up to 4374 V/cm at 0.25 mol%. The varistor ceramics doped with 0.05 mol% Nb_2O_5 exhibited the best nonlinear properties, in which the nonlinear coefficient is 47 and the leakage current density is 0.14 mA/cm^2.

Keywords: B. Grain boundaries; C. Electrical properties; D. ZnO; E. Varistors

1. Introduction

Crystalline zinc oxide (ZnO) is a useful material that possesses a wide range of applications as active component in optical and electrical devices. Polycrystalline ZnO ceramics are widely applied to varistors using grain boundary effect. ZnO varistors are *n*-type semiconductor devices formed by sintering ZnO powder with one additive, which is necessary to initiate the varistor effect, and minor subordinate additives, which are necessary to improve various varistor properties. They exhibit non-ohmic conduction characteristics with symmetric *V–I* curves analogous to a back-to-back Schottky diode [1,2]. Furthermore, they have greater pulse-current handling capabilities, due to 3-dimmensional multi-junction grain boundaries in the sintered ceramics. As a result, they have been extensively used to protect various semiconductor devices, electronic circuits, and electric power systems from dangerous transient voltages [2–4].

Today, commercial chip varistor ceramics can't be co-fired with a pure Ag (m.p. 961 °C) as an inner-electrode instead of expensive Pd or Pt alloy because of their high sintering temperature above 1000 °C. However, one candidate is $ZnO–V_2O_5$-based ceramics, which can be co-fired with a pure Ag as an inner-electrode in the vicinity of 900 °C [5]. At present, $ZnO–V_2O_5$-based ceramics are being studied for only chip varistors, unlike $ZnO–Bi_2O_3$- and $ZnO–Pr_6O_{11}$-based varistor ceramics, which have been used in many ways. A study of $ZnO–V_2O_5$-based ceramics is yet in its early stages in many points [6–17]. The specific additives and sintering process enable $ZnO–V_2O_5$-based ceramics to exhibit stronger nonlinear properties. Up to now, $ZnO–V_2O_5$-based ceramics modified with mainly MnO_2 has been studied [6–11,13,14,16]. However, the $ZnO–V_2O_5$-based ceramics modified with Mn_3O_4 were rarely studied [12,15,17]. In this study, Nb_2O_5 doping effect on microstructure and electrical properties of ternary $ZnO–V_2O_5–Mn_3O_4$ varistor ceramics was investigated and surprisingly high nonlinear coefficient (α) were obtained by proper amount of Nb_2O_5.

2. Experimental procedure

Reagent-grade raw materials with $(99.0 - x)$ mol% ZnO + 0.5 mol% V_2O_5 + 0.5 mol% Mn_3O_4 + x mol% Nb_2O_5 (x = 0.0, 0.025, 0.05, 0.1, and 0.25) were prepared. Raw materials were mixed by ball milling with zirconia balls and acetone in a polypropylene bottle for 24 h. The mixed slurry

* Tel.: +82 51 890 1669; fax: +82 51 890 1664.
E-mail address: cwnahm@deu.ac.kr.

0272-8842/$36.00
doi:10.1016/j.ceramint.2012.02.052

was dried at 120 °C for 12 h. The dried mixture was mixed by magnetic stir bar into a beaker with acetone and 0.8 wt.% polyvinyl butyral binder of powder weight. After drying, the mixture was granulated by sieving through a 100-mesh screen to produce starting powder. The sieved powder was pressed into disc-shaped pellet of 10 mm in diameter and 1.5 mm in thickness at a pressure of 100 MPa. The pellets were set on MgO plate into alumina sagger and sintered at 900 °C in air for 3 h, and furnace-cooled to room temperature. The heating and cooling rates were 4 °C/min. The final pellets were about 8 mm in diameter and 1.0 mm in thickness. Silver paste was coated by screen-printing techniques on both faces of the pellets and the electrodes were formed by heating it at 550 °C for 10 min. The electrodes were 5 mm in diameter. Finally, after the lead wire is soldered to both electrodes, the samples were packaged by dipping it into a thermoplastic resin powder.

Both surfaces of the sintered pellets were lapped and ground with SiC paper and polished with 0.3 μm-Al_2O_3 powders to a mirror-like surface. The polished pellets were chemically etched into $1HClO_4$:$1000H_2O$ for 25 s at 25 °C. The surface microstructure was examined using a field emission scanning electron microscope (FESEM, Quanta 200, FEI, Brno, Czech). The average grain size (d) was determined by the linear intercept method [18]. The crystalline phases were identified using an X-ray diffractometer (XRD, X′pert-PRO MPD, Panalytical, Almelo, Netherlands) with Cu K_α radiation. The

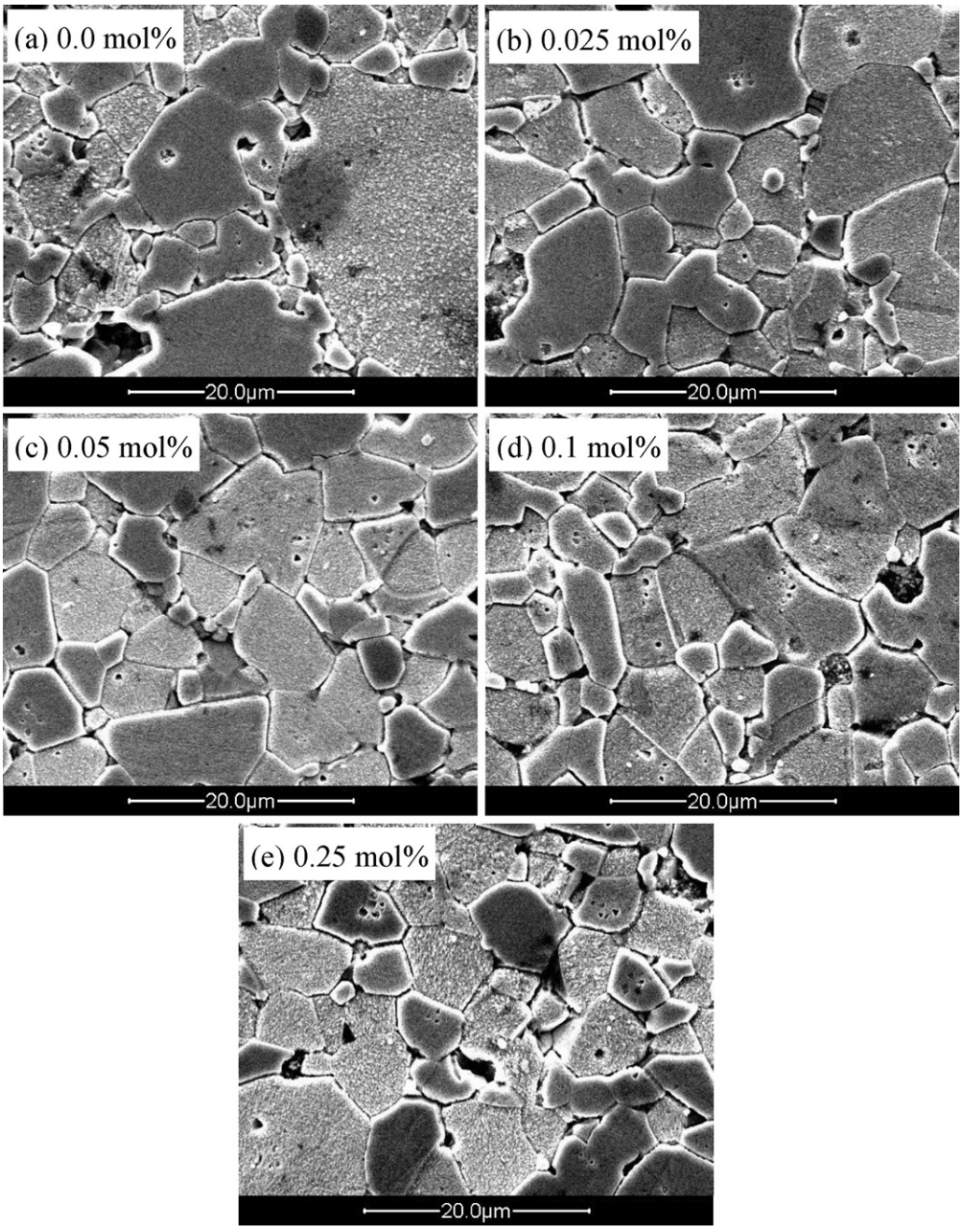

Fig. 1. SEM micrographs of the samples for different amounts of Nb_2O_5.

sintered density (ρ) was measured using a density determination kit (238490) attached to balance (AG 245, Mettler Toledo International Inc., Greifensee, Switzerland).

The electric field-current density (E–J) characteristics were measured using a V–I source (Keithley 237, Keithley Instruments Inc., Cleveland, OH, USA). The breakdown field (E_B) was measured at a current density of 1.0 mA/cm^2 and the leakage current density (J_L) was measured at 0.80 E_B. In addition, the nonlinear coefficient (α) was determined from $\alpha = (\log J_2 - \log J_1)/(\log E_2 - \log E_1)$, where E_1 and E_2 are the electric fields corresponding to $J_1 = 1.0$ mA/cm^2 and $J_2 = 10$ mA/cm^2, respectively.

3. Results and discussion

Fig. 1 shows the SEM micrographs of the samples with different amounts of Nb_2O_5. The addition of Nb_2O_5 has an effect on the surface morphology in the microstructure. The uniformity of grain size was improved with an increase in the amount of Nb_2O_5 up to 0.05 mol%. The average grain size increased in the range of 6.64–7.27 μm by the addition of Nb_2O_5, compared with it (6.44 μm) in the Nb_2O_5-free sample. On the whole, the average grain size has a fluctuation (see Fig. 4 in advance). The density of sintered pellets increased a little bit from 5.50 to 5.54 g/cm^3 corresponding to 95.1–95.8% of the theoretical density (TD) (pure ZnO, TD = 5.78 g/cm^3) with an increase in the amount of Nb_2O_5. This means the Nb-species may restrict the volatility of the V-species for V_2O_5 with low melting point. The microstructure parameters are summarized in Table 1.

The XRD patterns of the samples with different amounts of Nb_2O_5 are shown in Fig. 2. These patterns revealed the presence of $Zn_3(VO_4)_2$, ZnV_2O_4, V_2O_5, and Mn_3O_4 as minor secondary phases, which act as liquid-phase sintering aids, in addition to a major phase of hexagonal ZnO [16]. The revealed phases are identical to those in the samples without Nb_2O_5. No secondary phase related to Nb_2O_5 was detected. The detailed microstructure parameters are summarized in Table 1.

Fig. 3 shows the electric field-current density (E–J) characteristics of the samples with different amounts of Nb_2O_5. The varistor properties are featured by the nonlinear conduction characteristics, which do not follow ohm's law ($J = \sigma E$, where σ is conductivity) in the E–J relation. The characteristic curves are divided into two regions: one is a linear region which shows very high resistance before breakdown field and another is a nonlinear region which shows very low resistance after breakdown field. The E–J characteristic parameters obtained from E–J curves are summarized in Table 1.

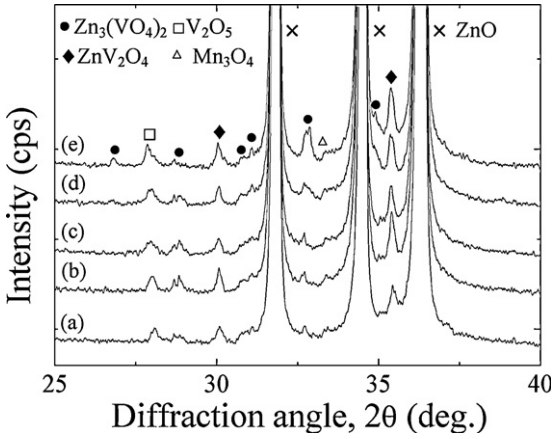

Fig. 2. XRD patterns of the samples for different amounts of Nb_2O_5: (a) 0.0 mol%, (b) 0.025 mol%, (c) 0.05 mol%, (d) 0.1 mol%, and (e) 0.25 mol%.

The behavior of breakdown field (E_B) as a function of Nb_2O_5 amount was indicated graphically in Fig. 4(c). The E_B decreased from 947 to 4521 V/cm with different amounts of Nb_2O_5 up to 0.1 mol%, as indicated in Fig. 4. The behavior of E_B in accordance with the amount of Nb_2O_5 can be explained by the grain size (d) and is the breakdown voltage per grain boundaries (v_{gb}). The varistors are devices depending on the thickness. The breakdown voltage (V_B) is sum of the breakdown voltage per grain boundaries (v_{gb}) in series between electrodes, and is defined as following equation: $V_B = (D/d)\cdot v_{gb} = n\cdot v_{gb}$, The above-expression is changed as follows: $E_B = v_{gb}/d$, where d is the average grain size, D is the thickness of sample, and n is the number of grain boundaries. Therefore, the V_B is proportional to n and v_{gb}. In general, to control the breakdown voltage, one can control the sample thickness for fixed grain size or alternately one can control the grain size for constant sample thickness. As a result, the increase of E_B with an increase in the amount of Nb_2O_5 is attributed to the increase of the average ZnO grain size and the increase of breakdown voltage per grain boundaries in the range of 0.6–3.0 V/gb. Further addition in the amount of Nb_2O_5 caused breakdown field to decrease to 4374 V/cm at 0.25 mol%. This is attributed to the decrease of average grain size and breakdown voltage per grain boundaries at 0.25 mol% Nb_2O_5.

The behavior of nonlinear coefficient (α) as a function of Nb_2O_5 amount was indicated graphically in Fig. 4(d). The α value increased from 20 to 47 with an increase in the amount of Nb_2O_5 up to 0.05 mol%. However, further addition in the amount of Nb_2O_5 caused nonlinear coefficient to decrease to 17

Table 1
Microstructure and E–J characteristic parameters of the samples for different amounts of Nb_2O_5.

Sample composition (all in mol%)	d (μm)	ρ (g/cm^3)	E_B (V/cm)	v_{gb} (V/gb)	α	J_L (mA/cm^2)
$ZnO + 0.5V_2O_5 + 0.5Mn_3O_4$	6.44	5.50	947	0.6	20	0.19
$ZnO + 0.5V_2O_5 + 0.5Mn_3O_4 + 0.025Nb_2O_5$	7.27	5.52	3518	2.5	27	0.32
$ZnO + 0.5V_2O_5 + 0.5Mn_3O_4 + 0.5Nb_2O_5$	6.91	5.52	3967	2.7	47	0.14
$ZnO + 0.5V_2O_5 + 0.5Mn_3O_4 + 0.1Nb_2O_5$	6.64	5.53	4521	3.0	21	0.34
$ZnO + 0.5V_2O_5 + 0.5Mn_3O_4 + 0.25Nb_2O_5$	6.67	5.54	4374	2.9	17	0.37

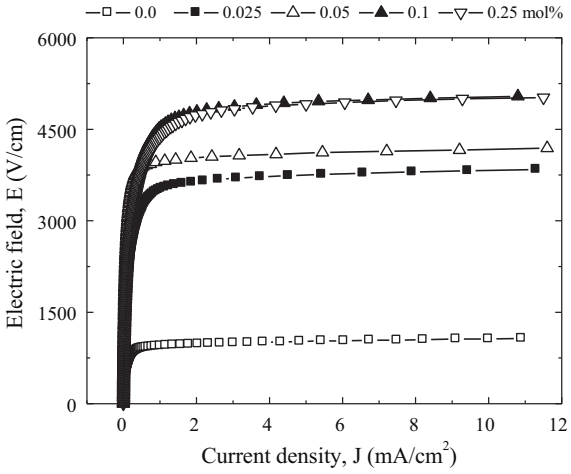

Fig. 3. *E–J* characteristics of the samples for different amounts of Nb_2O_5.

at 0.25 mol%. It should be noted that the sample modified with 0.05 mol% Nb_2O_5 exhibited the highest value ($\alpha = 47$) in the ZnO–V_2O_5-based varistors modified with Mn_3O_4 reported until now [12,15,17] and it is compared with the quaternary ZnO–V_2O_5-based varistors reported until now [19]. Therefore, this may be tuning point in the development of the ZnO–V_2O_5-based varistor ceramics for a high performance as a new composition. As a result, it can be seen that the incorporation of Nb_2O_5 has a significant effect on nonlinear properties. The behavior of α can be related to the potential barrier depending on the electronic states at the grain boundaries in accordance with the incorporation of Nb_2O_5. The Nb_2O_5 may vary the density of interface states with the transport of the defect ions toward the grain boundaries. Therefore, the increase or decrease of α with an increase in the amount of Nb_2O_5 is attributed to the increase or decrease of potential barrier height at the grain boundaries. The behavior of leakage current density

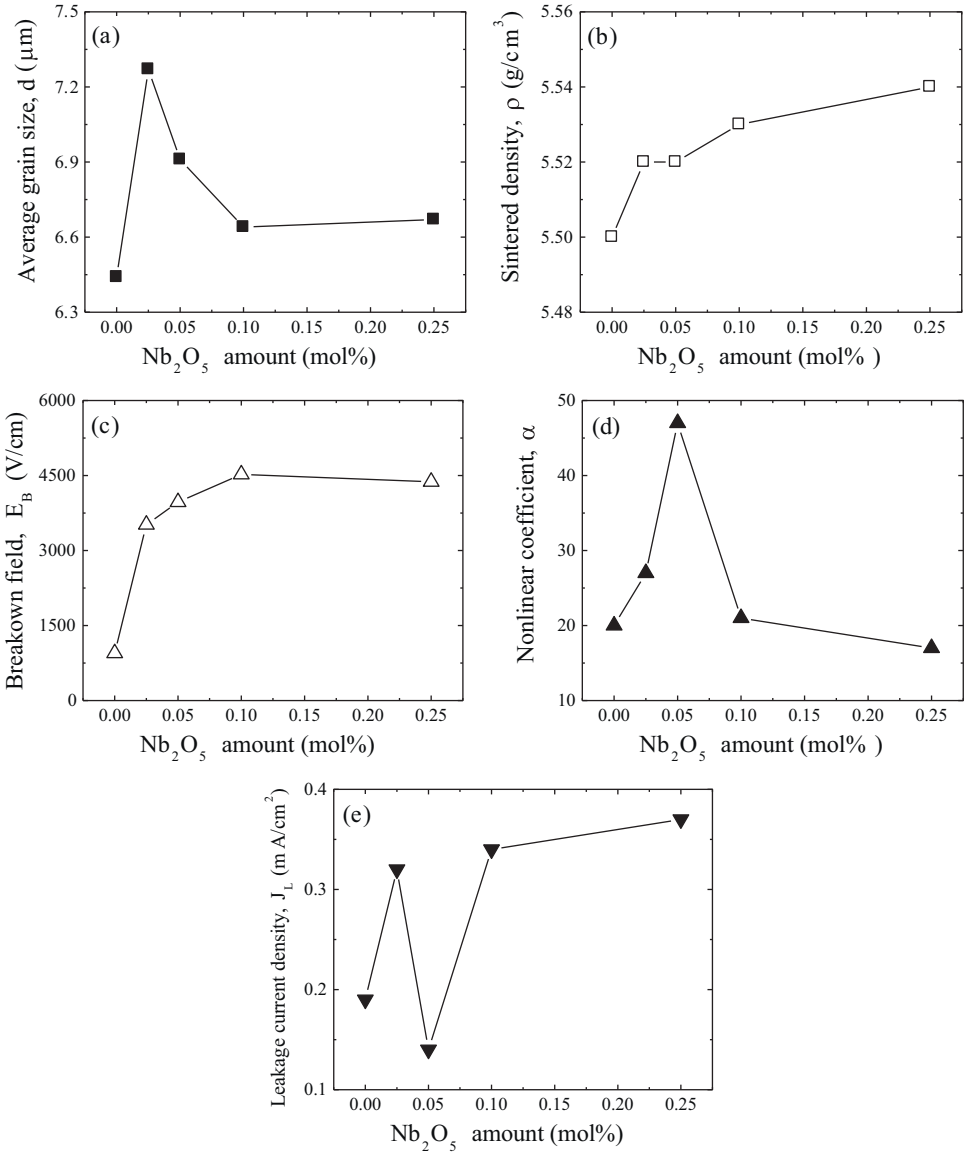

Fig. 4. Microstructure and electrical parameters of the samples as a function of Nb_2O_5 amount: (a) average grain size, (b) sintered density, (c) breakdown field, (d) nonlinear coefficient, and (e) leakage current density.

(J_L) as a function of Nb_2O_5 amount was indicated graphically in Fig. 4(e). The J_L value with an increase in the amount of Nb_2O_5 exhibited a minimum value (0.14 mA/cm^2) at 0.05 mol%. Further addition in the amount of Nb_2O_5 caused leakage current density to increase to 0.37 mA/cm^2 at 0.25 mol%.

4. Conclusions

The effect of Nb_2O_5 addition on microstructure and electrical properties of ternary ZnO–V_2O_5–Mn_3O_4 varistor ceramics were investigated. Experimental results indicated that doping effect has a significant effect on nonlinear properties. The sintered density of pellets increased with an increase in the amount of Nb_2O_5. However, the average grain size was found to have a fluctuation. As the amount of Nb_2O_5 increased, the breakdown field increased up to 0.1 mol% Nb_2O_5, whereas a further addition caused it to decrease. Considering nonlinear properties, optimum amount of Nb_2O_5 was 0.05 mol%, with 47 in the nonlinear coefficient and 0.14 mA/cm^2 in the leakage current density. Finally, it is believed that quaternary ZnO–$0.5V_2O_5$–$0.5Mn_3O_4$–$0.5Nb_2O_5$ (all in mol%) varistor ceramics can be applied as a new basic composition.

References

[1] M. Matsuoka, Nonohmic properties of zinc oxide ceramics, Jpn. J. Appl. Phys. 10 (1971) 736–746.

[2] H.R. Pilipp, L.M. Levinson, The physics of metal oxide varistors, J. Appl. Phys. 46 (1976) 1332–1341.

[3] L.M. Levinson, H.R. Philipp, Zinc oxide varistor—a review, Am. Ceram. Soc. Bull. 65 (1986) 639–646.

[4] T.K. Gupta, Application of zinc oxide varistor, J. Am. Ceram. Soc. 73 (1990) 1817–1840.

[5] J.-K. Tsai, T.-B. Wu, Non-ohmic characteristics of ZnO–V_2O_5 ceramics, J. Appl. Phys. 76 (1994) 4817–4822.

[6] J.-K. Tsai, T.-B. Wu, Microstructure and nonohmic properties of binary ZnO–V_2O_5 ceramics sintered at 900 °C, Mater. Lett. 26 (1996) 199–203.

[7] C.T. Kuo, C.S. Chen, I.-N. Lin, Microstructure and nonlinear properties of microwave-sintered ZnO–V_2O_5 varistors: I, effect of V_2O_5 doping, J. Am. Ceram. Soc. 81 (1998) 2942–2948.

[8] H.-H. Hng, K.M. Knowles, Microstructure and current–voltage characteristics of multicomponent vanadium-doped zinc oxide varistors, J. Am. Ceram. Soc. 83 (2000) 2455–2462.

[9] H.-H. Hng, P.L. Chan, Effects of MnO_2 doping in V_2O_5-doped ZnO varistor system, Mater. Chem. Phys. 75 (2002) 61–66.

[10] H.-H. Hng, P.L. Chan, Microstructure and current-voltage characteristics of ZnO–V_2O_5–MnO_2 varistor system, Ceram. Int. 30 (2004) 1647–1653.

[11] C.-W. Nahm, Microstructure and varistor properties of ZnO–V_2O_5–MnO_2-based ceramics, J. Mater. Sci. 42 (2007) 8370–8373.

[12] C.-W. Nahm, Improvement of electrical properties of V_2O_5 modified ZnO ceramics by Mn-doping for varistor applications, J. Mater. Sci. Mater. Electron. 19 (2008) 1023–1029.

[13] H.-H. Hng, P.L. Chan, Cr_2O_3 doping in ZnO–0.5 mol% V_2O_5 varistor ceramics, Ceram. Int. 35 (2009) 409–413.

[14] C.-W. Nahm, Effect of sintering temperature on varistor properties and aging characteristics of ZnO–V_2O_5–MnO_2 ceramics, Ceram. Int. 35 (2009) 2679–2685.

[15] C.-W. Nahm, Preparation and varistor properties of new quaternary Zn–V–Mn–(La, Dy) ceramics, Ceram. Int. 35 (2009) 3435–3440.

[16] C.-W. Nahm, Effect of dopant (Al, Nb, Bi, La) on varistor properties of ZnO–V_2O_5–MnO_2–Co_3O_4–Dy_2O_3 ceramics, Ceram. Int. 36 (2010) 1109–1115.

[17] C.-W. Nahm, Varistor properties and aging behavior of ZnO–V_2O_5–Mn_3O_4 ceramics with sintering process, J. Mater. Sci. Mater. Electron. 22 (2011) 1010–1015.

[18] J.C. Wurst, J.A. Nelson, Lineal intercept technique for measuring grain size in two-phase polycrystalline ceramics, J. Am. Ceram. Soc. 55 (1972) 109–111.

[19] C.-W. Nahm, Sintering effect on electrical properties of ZnO–V_2O_5–MnO_2–Nb_2O_5 ceramics, J. Alloy Compd. 509 (2011) L314–L317.